Journal Pre-proof

JNK-JUN-NCOA4 axis contributes to chondrocyte ferroptosis and aggravates osteoarthritis via ferritinophagy

Kai Sun, Liangcai Hou, Zhou Guo, Genchun Wang, Jiachao Guo, Jingting Xu, Xiong Zhang, Fengjing Guo

PII: S0891-5849(23)00106-5

DOI: https://doi.org/10.1016/j.freeradbiomed.2023.03.008

Reference: FRB 15976

To appear in: *Free Radical Biology and Medicine*

Received Date: 3 February 2023

Revised Date: 3 March 2023

Accepted Date: 7 March 2023

Please cite this article as: K. Sun, L. Hou, Z. Guo, G. Wang, J. Guo, J. Xu, X. Zhang, F. Guo, JNK-JUN-NCOA4 axis contributes to chondrocyte ferroptosis and aggravates osteoarthritis via ferritinophagy, *Free Radical Biology and Medicine* (2023), doi: https://doi.org/10.1016/j.freeradbiomed.2023.03.008.

JNK-JUN-NCOA4 axis contributes to chondrocyte ferroptosis and aggravates osteoarthritis via ferritinophagy

Kai Sun[1], Liangcai Hou[1], Zhou Guo[1], Genchun Wang[1], Jiachao Guo[2], Jingting Xu[1], Xiong Zhang[1], Fengjing Guo[1,*]

[1]Department of Orthopedics, Tongji Hospital, Tongji Medical College, Huazhong University of Science and Technology, Wuhan, Hubei 430030, China.

[2]Department of Pediatric Surgery, Tongji Hospital, Tongji Medical College, Huazhong University of Science and Technology, Wuhan, Hubei 430030, China.

*Corresponding author:

Fengjing Guo, Department of Orthopedics, Tongji Hospital, Tongji Medical College, Huazhong University of Science and Technology, Wuhan, Hubei 430030, China.

Tel./ Mobile Number: +86-27-8366 5238

Fax: +86-27-8366-3670

E-mail: guofjdoc@163.com

Authors' Information:

Kai Sun: 1085844308@qq.com

Liangcai Hou: 847442475@qq.com

Zhou Guo: 1178519539@qq.com

Genchun Wang: 455703865@qq.com

Jiachao Guo: 793527829@qq.com

Jingting Xu: JT.Xu@hotmail.com

Xiong Zhang: zhangxiong1123@qq.com

Fengjing Guo: guofjdoc@163.com

Declarations of interest: none.

Running title: JNK-JUN-NCOA4 axis in osteoarthritis pathogenesis

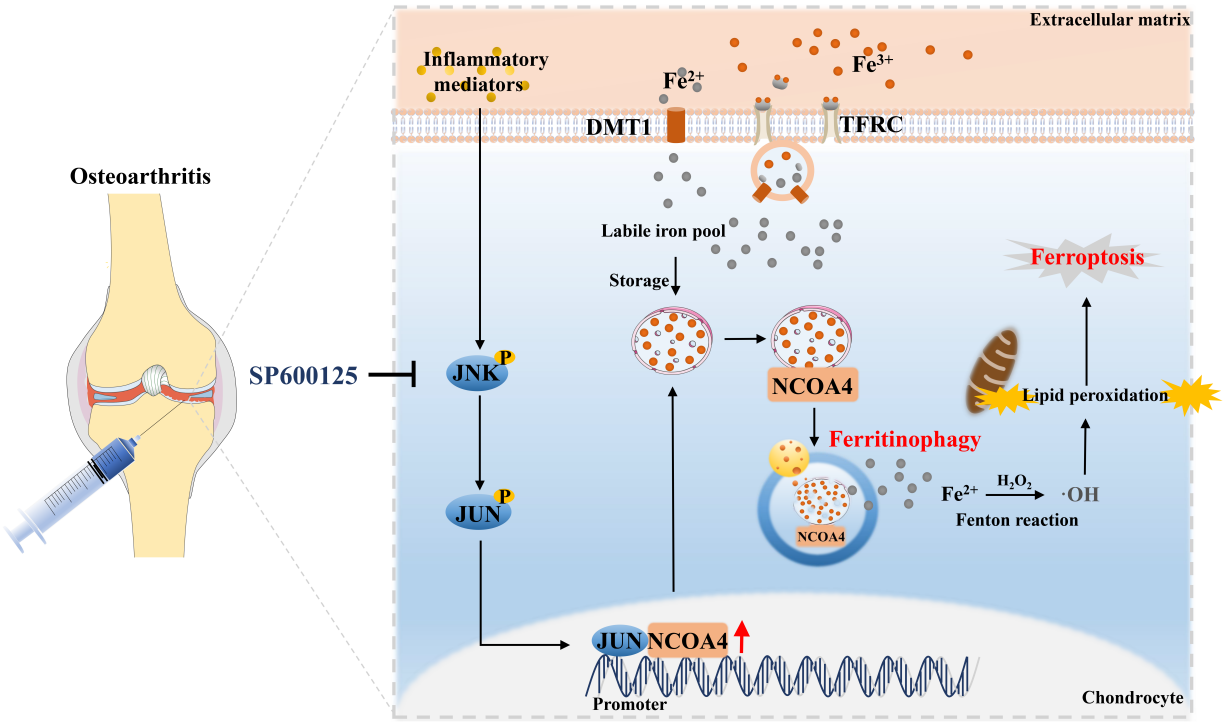
Osteoarthritis
SP600125
Extracellular matrix
Inflammatory mediators
Fe2+
Fe3+
DMT1
TFRC
Labile iron pool
Storage
JNK
P
JUN
P
NCOA4
Ferroptosis
Lipid peroxidation
Ferritinophagy
Fe2+
H2O2
·OH
Fenton reaction
NCOA4
JUN
NCOA4
Promoter
Chondrocyte

JNK-JUN-NCOA4 axis contributes to chondrocyte ferroptosis and aggravates osteoarthritis via ferritinophagy

Running title: JNK-JUN-NCOA4 axis in osteoarthritis pathogenesis

Abbreviations:

3-MA: 3-methyladenine; AAV9: Adreno-Associated Virus 9; ACSL4: Acyl-CoAsynthetase long chain family member 4; ADAMTS5: ADAM metallopeptidase with thrombospondin type 1 motif 5; BafA1: bafilomycin A1; BV/TV: Bone volume/total volume; CCK8: cell counting kit-8; ChIP: chromatin immunoprecipitation; Co-IP: Co-immunoprecipitation; COL2A1: collagen type II alpha 1 chain; COX2: cyclooxygenase-2; DMM: destabilisation of the medial meniscus; ECM: extracellular matrix; FTH1: ferritin heavy chain 1; GPX4: glutathione peroxidase 4; GSH: glutathione; HBSS: Hank's Balanced Salt Solution; H&E: hematoxylin-eosin; IF: immunofluorescence; IHC: immunohistochemistry; IL-1β: interleukin-1β; iNOS: inducible nitric oxide synthase; JNK: c-Jun N-terminal kinase; MAP1LC3B/LC3: Microtubule-associated protein 1 light chain 3 beta; MDA: malondialdehyde; MMP3: matrix metallopeptidase 3; MMP13: matrix metallopeptidase 13; NC: negative control; NCOA4: nuclear receptor coactivator 4; OA: osteoarthritis; OARSI Osteoarthritis Research Society International; Rapa: rapamycin; ROS: reactive oxygen species; siRNA small interfering RNA; TBHP: Tert-butyl hydroperoxide; Tb.N: Trabecular number; Tb.Sp: Trabecular separation; Tb.Th: Trabecular thickness; TEM: transmission electron microscopy; TFs: transcription factors.

Abstract

Interruption of iron homeostasis is correlated with cell ferroptosis and degenerative diseases. Nuclear receptor coactivator 4 (NCOA4)-mediated ferritinophagy has been reported as a vital mechanism to control cellular iron levels, but its impact on osteoarthritis (OA) pathology and the underline mechanism are unknown. Herein we aimed to investigate the role and regulatory mechanism of NCOA4 in chondrocyte ferroptosis and OA pathogenesis. We demonstrated that NCOA4 was highly expressed in cartilage of patients with OA, aged mice, post-traumatic OA mice, and inflammatory chondrocytes. Importantly, *Ncoa4* knockdown inhibited IL-1β-induced chondrocyte ferroptosis and extracellular matrix degradation. Contrarily, overexpression of NCOA4 promoted chondrocyte ferroptosis and the delivery of *Ncoa4* adeno-associated virus 9 into knee joint of mice aggravated post-traumatic OA. Mechanistic study revealed that NCOA4 was upregulated in a JNK-JUN signaling-dependent manner in which JUN could directly bind to the promoter of *Ncoa4* and initial the transcription of *Ncoa4*. NCOA4 could interact with ferritin and increase autophagic degradation of ferritin and iron levels, which caused chondrocyte ferroptosis and extracellular matrix degradation. In addition, inhibition of JNK-JUN-NCOA4 axis by SP600125, a specific inhibitor of JNK, attenuated development of post-traumatic OA. This work highlights the role of JNK-JUN-NCOA4 axis and ferritinophagy in chondrocyte ferroptosis and OA pathogenesis, suggesting this axis as a potential target for OA treatment.

Keywords: chondrocyte; ferritinophagy; ferroptosis; JUN; NCOA4; osteoarthritis (OA).

Chemical compounds studied in this article: 3-methyladenine (PubChem CID:

135398661); Rapamycin (PubChem CID: 5284616); 1,9-Pyrazoloanthrone/SP600125 (PubChem CID: 8515); bafilomycin A1 (PubChem CID: 6436223).

Introduction

The etiology of osteoarthritis (OA) is complex and exact molecular mechanism of OA pathogenesis is largely unknown. Previous studies have reported that iron level is significantly increased in the joint fluid of OA patients[1], and the level of serum ferritin in OA patients is positively correlated with the degree of knee cartilage injury[2]. The recent study has found that systemic iron overload can cause iron accumulation in joints of guinea pig and lead to joint degeneration[3]. These findings suggest that abnormal iron accumulation is closely correlated to the development of OA. Iron is an essential element for human body and participates in multiple cellular processes, such as hemoglobin synthesis, electron transport, cell respiration and so on[4]. Intracellular iron homeostasis is precisely regulated by iron metabolism system and maintenance of cellular iron homeostasis is essential for the function and fate of cells[4].

The abnormal accumulation of iron ions within cells can cause lipid peroxidation via Fenton reaction and trigger an iron dependent type of cell death-ferroptosis[5]. In view of the close relationship between ferroptosis and cellular oxidation level, more and more studies focus on the role of ferroptosis in ageing related diseases and results from these studies highlight the importance of ferroptosis during pathogenesis of Parkinson's disease[6], macular degeneration[7], and retinal pigment epithelium degeneration[8]. Therefore, targeting ferroptosis has become a potential therapeutic approach for these diseases[9]. Previous studies have found that chondrocytes have a

variety of characteristics of ferroptosis under pathological conditions: abnormal iron metabolism[10], lipid peroxidation[11], and mitochondrial dysfunction[12]. Our previous studies have found that inflammatory environment or iron overload environment could lead to ferroptosis of chondrocytes[13]. We also found that the specific inhibitor of ferroptosis, Ferrostatin 1, and iron chelator, Deferoxamine, could reduce chondrocyte ferroptosis and delay the progression of OA in mice[13,14]. Additionally, the transcriptomic, biochemical, and microscopical analyses have indicated that ferroptosis is closely associated with OA[15]. These evidence confirms that chondrocyte ferroptosis is involved in the progression of OA. However, the regulatory mechanism of chondrocyte ferroptosis is largely unknown.

Nuclear receptor coactivator 4 (NCOA4) is a selective cargo receptor for the autophagic turnover of ferritin in lysosomes and this recycling process is termed ferritinophagy[16]. Ferritinophagy is implicated in a variety of pathological processes. Masahiro Yoshida et al. have found that smoke exposure can stimulate the expression of NCOA4, continuously activate autophagic degradation of ferritin, further cause the accumulation of iron ions in bronchial epithelial cells and toxic reactions, leading to the occurrence and development of chronic obstructive pulmonary disease in mice[17]. These studies establish a new relationship between cellular iron homeostasis and the pathogenesis of iron associated diseases. As NCOA4 is widely expressed in mammalian cells, its function may have an effect on a variety of diseases. However, the relationship and role of NCOA4 in OA progression have not been reported.

In the present study, we examined the expression pattern of NCOA4 in OA chondrocyte, and investigated the role of NCOA4 in chondrocyte ferroptosis and OA

pathogenesis. We also investigated that whether NCOA4-mediated ferritinophagy is involved in chondrocyte ferroptosis. In addition, we sought to explore the regulatory mechanism of NCOA4 expression and determined whether inhibition of c-Jun N-terminal kinase (JNK)-JUN-NCOA4 axis could slow the progression of OA.

Materials and methods

Human samples

The collection of human cartilage samples was approved by the Ethics Committee of Tongji Hospital (TJ-IRB20210905). Informed consent was obtained from all participants. Control cartilage was collected from four amputees without a history of OA, and OA cartilage was obtained from OA patients after total knee replacement surgery at the Tongji Hospital (n = 12). The information of OA patients and amputees is shown in Table S1 and Table S2.

Materials and reagents

Recombinant Mouse interleukin 1 beta (IL-1β) (401-ML-010/CF) was obtained from R&D Systems. The tert-Butyl hydroperoxide (TBHP) (458139), Deferoxamine (D9533), dimethylsulfoxide (D8418) were purchased form Sigma-Aldrich. 3-methyladenine (3-MA) (S2767), SP600125 (S1460) and rapamycin (Rapa) (S1039) were purchased from Selleck and diluted in DMSO. Bafilomycin A1 (BafA1) (MB5505) was obtained from meilunbio.

Chondrocyte isolation, and culture

Chondrocytes were isolated from 5-day-old C57BL/6J mice. In brief, removed from the knee joints, cartilage was cut into pieces and then digested with 0.25%

trypsin for 30 minutes. After that, the pieces were further digested with 0.25% type 2 collagenase for 4-6 h. The cells were resuspended and cultured in DMEM/F12 medium with 10% fetal bovine serum, 1% streptomycin sulfate and 1% penicillin at 37°C. Only the first or second passages of chondrocytes were used in the experiments.

Cell viability assays

Cell viability was determined using a cell counting kit assay (CCK-8) (MedChemExpress, HY-K0301). Briefly, chondrocytes were seeded into 96-well plates (about 5,000 cells/well) allowing adherence for 24 h and then treated as the figure legend indicated. After 72 h, the medium of each well was replaced by 100 μl of culture solution and 10 μl of CCK-8 was added to each well. After one-hour incubation, absorbance was measured using a microplate reader at the wavelength of 450 nm.

Small interfering RNA (siRNA), Plasmids and transfection

The siRNAs against *Ncoa4*, *Fth1*, *Jun* and negative control siRNA were synthesized by RiboBio. The siRNA sequence was as follows: si-*Ncoa4* 1#: CCACATTTGGATCCCTTAA; si-*Ncoa4* 2#: CTACAAGAAGAACGTAACT; si-*Ncoa4* 3#: CCAGTTCTTTCTCTCCTGA; si-*Fth1* 1#: TGGCTACTGACAAGAAT GA; si-*Fth1* 2#: CCGAGAAACTGATGAAGCT; si-*Fth1* 3# ACACGGTGATGAGA GCTAA. Si-*Jun* 1#: CCAAGAACTCGGACCTTCT; si-*Jun* 2#: GGCACAGCTTAA GCAGAAA; si-*Jun* 3#: GCCAACTCATGCTAACGCA. When reaching 60–70% of confluence, murine chondrocytes were transfected with 50 nmol siRNA using Lipofectamine 3000 (Invitrogen, L3000015) according to the manufacture's instruction. Flag-tagged plasmid of *Ncoa4* and negative control plasmid were

synthesized by Vigene Biosciences. The construct was confirmed by DNA sequencing. When reaching 60–70% of confluence, the cells were transfected with 1 μg purified plasmid using Lipofectamine 3000.

Measurement of lipid peroxidation

Cells were washed twice with basic medium and loaded with 1000 X C11 BODIPY solution (Thermo Fisher, D3861) for 30 min at 37℃ in the dark. After that, the cells were washed with basic medium for 5 times and then excited using the 488 and 565 nm laser of fluorescence microscope. Oxidation of the polyunsaturated butadienyl portion of C11-BODIPY causes a shift of the fluorescence emission peak from 590 nm to 510 nm, which reflects lipid peroxidation in membranes The fluorescence was measured by emission wavelength of 590 nm and 510 nm and then. was merged, and intensity of green fluorescence in merge image indicates the level of lipid peroxidation.

Measurement of malonaldehyde (MDA) and glutathione (GSH)

After the indicated treatment for 48 h, the levels of MDA and GSH in cell lysates were measured with MDA Assay Kit (Beyotime, S0131S) and GSH detection kit (Beyotime, S0053) according to the manufacturer's instruction. The measurement was based on the absorbance of specific substrates and performed using microplate reader.

In vivo overexpression of NCOA4 using adeno-associated virus

Adeno-associated virus 9 containing *Ncoa4* (AAV9-NCOA4) (Vigene Biosciences) was administered to 8-week C57BL/6J mice by intra-articular injection. Knee joints were collected at 2 weeks, 6 weeks, and 10 weeks post the first injection

for examining transfection efficiency of AAV9 and expression level of NCOA4. The doses (10 μl, 1×10^{12} vg/ml) of AAV9 joint injection were chosen as previously reported[18]. Two weeks after the AAV9 joint injection, the destabilisation of the medial meniscus (DMM) surgery or sham operation was performed. Knee joints were collected 8 weeks post-surgery for histological analyses. The groups that did not need injection of AAV9-NCOA4 were all treated with negative control (AAV9-GFP) for the same periods.

Animals experiment

Adult male C57BL/6 mice (eight weeks of age) were used for *in vivo* experiments. All animal experiments were approved by the institutional Animal Care and Use Committee at Tongji Medical Collage, Huazhong University of Science and Technology. After anesthetized by intraperitoneal injection of pentobarbital (35 mg/kg), The DMM surgery was performed to induce post-traumatic OA following the instructions described previously[19]. As the control, the medial knee joint capsule was incised for sham operation. We randomly divided mice into four groups with 9 mice per group: SHAM + AAV9-GFP, SHAM + AAV9-NCOA4, DMM + AAV9-GFP, and DMM + AAV9-NCOA4 groups. For *in vivo* experiment of SP600125 administration, we randomly divided mice into three groups with 6 mice per group: DMM + AAV9-GFP, DMM + AAV9-GFP + SP600125, and DMM + AAV9-NCOA4 + SP600125. 10 μl of SP600125 (1 mg/kg) or vehicle solution was injected articularly once per week for 7 weeks.

Western blot analysis

Cells were lysed in RIPA buffer with a protease inhibitor cocktail for 15 min on

ice followed by 30 minutes centrifugation at 12000 g. Protein concentration was measured using a bicinchoninic acid assay kit (Boster, AR1110). Equal amounts of total protein (20 μg) were mixed with loading buffer, boiled at 100°C for 10 min. The protein samples were separated by SDS-PAGE and transferred to polyvinyl difluoride membranes (Millipore, USA). Membranes were blocked with 5% milk without fat solved in 1 X TBST (Boster, AR0144) for 1 h and then incubated with various primary antibodies, including NCOA4 (Abcam, ab86707; diluted at 1: 1000), LC3 (Cell Signaling Technology, 4108; 1: 1000), FTH1 (Abcam, ab75973; 1: 1000), ACSL4 (Abcam, ab155282; 1: 1000), P53 (Cell Signaling Technology, 2524; 1: 1000), GPX4 (Abcam, ab125066; 1: 1000), COL2A1 (Proteintech, 15943-1-AP; 1: 800), ADAMTS5 (Boster, BA3020; 1: 300), iNOS (Cell Signaling Technology, sc-7271; 1: 1000), COX2 (Cell Signaling Technology, 12882; 1: 1000), MMP3 (Boster, BM4074; 1: 500), MMP13 (Abcam, ab39012; 1: 1000), Phospho-JNK (Cell Signaling Technology, 4668; 1: 1000), and Phospho-CJUN (Cell Signaling Technology, 3270; 1: 1000) overnight at 4°C. After washing the membranes in TBST four times (7 min/time), anti-rabbit or anti-mouse secondary antibody was diluted at 1:5000 with TBST, in which the membranes were incubated for 1 h. GAPDH (Proteintech, 60004-1-Ig) or β-ACTIN (Proteintech, 20536-1-AP) at a 1:10000 dilution was used as the internal control. The signal intensity of the membranes was visualized by a Bio-Rad scanner (Bio-Rad, Hercules, CA).

Quantitative RT-PCR

RNA was isolated using a total RNA (1 μg) extraction kit (Omega Biotek, R6834-01). Complementary DNA was synthesized using a Hifair® III 1st Strand cDNA Synthesis SuperMix (Yeasen, 11141ES60). SYBR Green Master Mix (Yeasen,

11203ES03) was used to amplify the cDNA. The amplification conditions utilized were as follows: 95℃ 5 min followed by 40 cycles of 10 seconds 95℃ and 30 seconds 60℃; 15 seconds 95℃, 60 seconds 60℃ and 15 seconds 95℃ for melt curve. GAPDH was used as an internal reference. Sequences of the primers of the indicated genes were as follows: *Ncoa4* (F) 5'-GCCCTACAATGTGAGTGATTGG-3', (R) 5'-ACTGGTGCAAGGCTCGTTG-3'. *Fth1* (F) 5'-CAAGTGCGCCAGAACTACCA-3', (R) 5'-GCCACATCATCTCGGTCAAAA-3', *Gapdh* (F) 5'-TGGATTTGGACGCATTGGTC-3', (R) 5'-TTTGCACTGGTACGTGTTGAT-3'. Each cDNA sample was repeated in triplicate.

Transmission electron microscopy (TEM) assays

TEM was used to observe morphological changes of mitochondria in chondrocytes. In brief, chondrocytes were washed with PBS (Boster, AR1155), and then fixed by electron microscope fixing solution (Servicebio, G1102), dehydrated with different concentrations of alcohol and acetone. After that, the samples were rinsed with propylene oxide and impregnated with epoxy resin. Ultrathin sections were stained with 1% uranyl acetate and 0.1% lead citrate. The Hitachi TEM system at an accelerating voltage of 80 kV was used for scanning.

Co-immunoprecipitation (Co-IP) assay.

The primary chondrocytes were cultured in 10 cm dishes and then treated with IL-1β for 12 h. Afterwards, cells were lysed with IP lysis buffer and supersound spallation (amplitude: 40%, pulse on 3 sec, pulse off 3 sec, total four cycles). The supernatant was collected by centrifugation at 12000 g for 15 min. Protein A/G Magnetic Beads (MedChemExpress, HY-K0202) were added into lysate to preclear

for 30 min at 4°C. Anti-NCOA4 antibody were used to form immune complexes with NCOA4 protein in lysates overnight at 4°C. Then the Protein A/G Magnetic Beads were added into lysates for 2 h at 4°C and then washed five times with lysis buffer, and bound proteins were eluted in 5 X loading buffer and denatured by boiling. equivalent protein samples were used for western blot analysis.

In vitro Safranin O staining

The Safranin O staining was used to observe morphology of chondrocyte and content of proteoglycan. In brief, chondrocytes were fixed in 4% paraformaldehyde for 15 min and washed by PBS. Next, the Safranin O solution was used to stain chondrocytes for 20 min. After that, the cells were washed by PBS three times and images were captured by a microscope (Evos Fl Auto, Life Technologies, USA).

Immunofluorescence (IF) staining

Chondrocytes were grown on 12-well culture slides and were pre-treated with bafilomycin A1 for 1 h and then treated with or without IL-1β for 6 h. The cells were then fixed with 4% paraformaldehyde for 15 min followed by permeabilization with 0.1% Triton X-100 (Sigma-Aldrich, T8787) for 5 min, and then blocked with 5% bovine serum albumin solved in TBST for 1 h. The anti-FTH1 (Abcam, ab75973; rabbit mAb; diluted at 1:100) and anti-LC3 (Cell Signaling Technology, 98557; mouse mAb; 1:100) primary antibodies and the corresponding second antibodies were used to incubate cells. After incubation, the cells were washed and labeled with DAPI (Boster, AR1177) for 5 min. The combination between FTH1 and LC3 proteins was scanned by fluorescence microscopy (OLYMPUS BX51, Japan).

mRFP-GFP-LC3 double-labelled adenovirus transfection

The mRFP-GFP-LC3 adenovirus was purchased from (Hanbio Biotechnology, HB-AP210 0001). Chondrocytes were seeded onto the slide, ensuring that the cell density will be about 50% in 24 h. After the transfection, the mRFP-GFP-LC3 adenovirus (MOI = 400) was added into the medium for 2 h and then replaced by fresh medium. After 24 h of incubation, the cells were treated with IL-1β for 12 h and then fixed with 4% paraformaldehyde. Cells were detected with green (GFP) or red (mRFP) fluorescence that was observed by FV3000 confocal microscope (Olympus, Japan). Autophagolysosome was formed by the fusion of autophagosome and lysosome, which results in acidic environment, causing the quenching of GFP fluorescence. At this time, only red fluorescence can be observed in the merged images. Therefore, red spots indicate autophagolysosomes and yellow spots (overlapped by green and red fluorescence) indicate autophagosomes. Autophagic flux was determined by increased red puncta in the merged images.

Chromatin immunoprecipitation (ChIP) assay and ChIP-PCR

ChIP assays were conducted with a ChIP assay kit (Beyotime, P2078) as previously described[20]. Briefly, chondrocytes were cross-linked with formaldehyde and chromatin fragmentation was carried out according to the protocol. The prepared chromatin solution was incubated with the JUN antibody overnight at 4°C. Normal rabbit IgG was used as negative control. After that, the above solution was incubated with protein A + G agarose beads. After the wash according to the protocol, the protein-DNA complexes were obtained and the eluted DNA was next subjected to ChIP-PCR. The primers used in the ChIP assay were as follows: F1, 5′-GGGTCAGTTAGGTGTGGCAT-3′; R1, 5′-AGTGACTAAGACAAGGCTGATGGG

C-3′; F2, 5′-ACCCCAACAAGGACACTCACTCTAA -3′; R2, 5′-CTTTTTTTCCTC TGGGGTTTGTGGT-3′; F3, 5′-TCTTACTCAAACCACCACAAACCCC-3′; R3, 5′-GGCTCACAACCACCCATACCTCCTG-3′. PCR amplifications were performed at 94°C for 1 min, followed by 40 cycles at 94°C for 30 s, 62°C for 30 s, 72°C for 1 min and then 72°C for 10 min.

Ferrous iron detection

After washed with Hank's Balanced Salt Solution (HBSS) three times, cells were stained in 1 μM Ferro orange (Dojindo, F374) in HBSS for 40 min at 37°C. Next, the cells were washed with HBSS three times and then imaged using fluorescence microscope (Evos fl auto, Life Technologies, USA).

Histological analyses

Tissue samples were fixed in 4% paraformaldehyde for 24 h. Specimens were decalcified with 10% EDTA (pH 7.4) for 21 days, embedded in paraffin and 5-μm thick sagittal sections were cut. Hematoxylin-eosin (H&E) and Safranin O/Fast green staining were performed according to standard protocols. Each section was assessed by two blinded researchers.

Safranin O/Fast green staining slides were used to evaluate cartilage degeneration by Osteoarthritis Research Society International (OARSI) scoring system. For OARSI scoring system, the 0-6 subjective scoring system was applied to evaluate severity of cartilage degeneration in medial femoral condyle and medial tibial plateau. 0 represents normal cartilage, 0.5 = loss of proteoglycan with an intact surface, 1 = superficial fibrillation without loss of cartilage, 2 = vertical clefts and loss of surface

lamina, 3 = vertical clefts/erosion to the calcified layer lesion for 1-25% of the quadrant width, 4 = lesion reaches the calcified cartilage for 25-50% of the quadrant width, 5 = lesion reaches the calcified cartilage for 50-75% of the quadrant width, 6 = lesion reaches the calcified cartilage for >75% of the quadrant width, the OA severity is expressed as maximal score[21].

Osteophyte size were scored on the anteromedial tibia in each sample stained by Safranin O/Fast green. Osteophyte size: 0 = none, 1 = small (approximately the same thickness as the adjacent cartilage), 2 = medium (~1–3 times the thickness of the adjacent cartilage), and 3 = large (~3 times the thickness of the adjacent cartilage)[22].

H&E slides were used to evaluate synovitis by scoring enlargement of the synovial lining cell layer and cellular density in the synovial stroma (score from 0 to 6). The synovial lining cell layer: 0 point = 1-2 lining cell layers; 1 point = 3-4 lining cell layers; 2 points = 5-9 lining cell layers, 3 points = ≥10 lining cell layers[23]. Density of the resident cells: 0 point = the synovial stroma shows normal cellularity, 1 point = the cellularity is slightly increased, 2 points = the cellularity is moderately increased, 3 points = the cellularity is greatly increased, multinucleated giant cells, pannus formation and rheumatoid granulomas might occur[23].

Micro-computed tomography (micro-CT) analysis

The left knee joints were fixed with 4% paraformaldehyde and then were evaluated via micro-CT using a Viva CT 80 scanner (Scanco Medical AG, Switzerland). Joints were scanned at 100 kV and 98 μA with the resolution of 10.5 μm. The reconstructed 3-dimensional (3D) images were acquired by Scanco Medical

software. The size of osteophytes was observed and calculated using the transverse sectional images of tibial plateau. The subchondral bone analysis of medial femoral condyle begins by starting at the distal 15 layers from edge of the tibial plateau until 30 layers were analyzed by two blinded observers. All non-cortical bone is included. The parameters of the trabeculae, including bone volume/tissue volume (BV/TV), trabecular numbers (Tb.N), trabecular thickness (Tb.Th), and trabecular space (Tb.Sp) were analyzed by the software in the μ-CT system.

Statistical analysis

For parametric test, Student's t-test and analysis of variance (ANOVA) test followed by Tukey's post hoc test were used for comparison between two different group or among multiple comparisons respectively. Mann-Whitney U test for two comparisons and Kruskal-Wallis test for multiple comparisons were used for nonparametric data. Data are presented as the mean ± SD. All statistical tests were conducted using GraphPad Prism 8.0 program. $P < 0.05$ was defined as significant, * means $P < 0.05$, ** means $P < 0.01$ while NS represents not significant.

Results

OA was characterized by altered expression of NCOA4

To determine the correlation between the expression of NCOA4 and OA progression, we examined the expression of NCOA4 in clinical OA samples and OA models. Severe cartilage degeneration was found in articular cartilage of patients with OA (Fig. 1A) and Immunohistochemistry (IHC) results showed that more NCOA4-expressing chondrocytes were observed in articular cartilage of patients with OA compared with the normal (Fig. 1B-C). In addition, aging is independent risk factor of

OA[24], we investigate expression pattern of NCOA4 in aged mice. Firstly, cartilage degeneration was confirmed in middle-aged (14-month-old) and aged (22-month-old) mice with higher OARSI scores compared to that of young mice (2-month-old) (Fig. 1D-E). It was further found that NCOA4-positive cells were markedly increased in cartilage of middle-aged and aged mice compared with that of young mice (Fig. 1F-G). Post-traumatic OA model is characterized by chronic mild inflammation, joint bleeding, and cartilage degeneration[25]. We performed DMM surgery to induce post-traumatic OA model of mouse and found that NCOA4-positive chondrocytes were significantly elevated in the cartilage of DMM model compared with that of sham control (Fig. 1H-I). We subsequently isolated primary murine chondrocytes (Fig. 1J) and examined the expression level of NCOA4 *in vitro*. Pro-inflammatory factors and oxidative stress are closely involved in OA pathogenesis[24]. Thereby, we used IL-1β to mimic inflammatory condition and used TBHP to induce oxidative stress condition in OA. The results showed that the protein expression of NCOA4 was upregulated in chondrocytes by the IL-1β or TBHP treatment accompanied by increased expression ratio of microtubule-associated protein 1 light chain 3 beta (LC3) II/I (Fig. 1K, L, N, O). The IF staining result confirmed an increased expression of NCOA4 in chondrocytes treated with IL-1β (Fig. 1M). Collectively, these results showed that NCOA4 expression was increased in the articular cartilage of patients with OA, aged mice and post-traumatic OA mice. Its expression was also promoted in response to pathologic conditions (IL-1β or TBHP). These findings suggest a positive correlation between NCOA4 expression and OA progression.

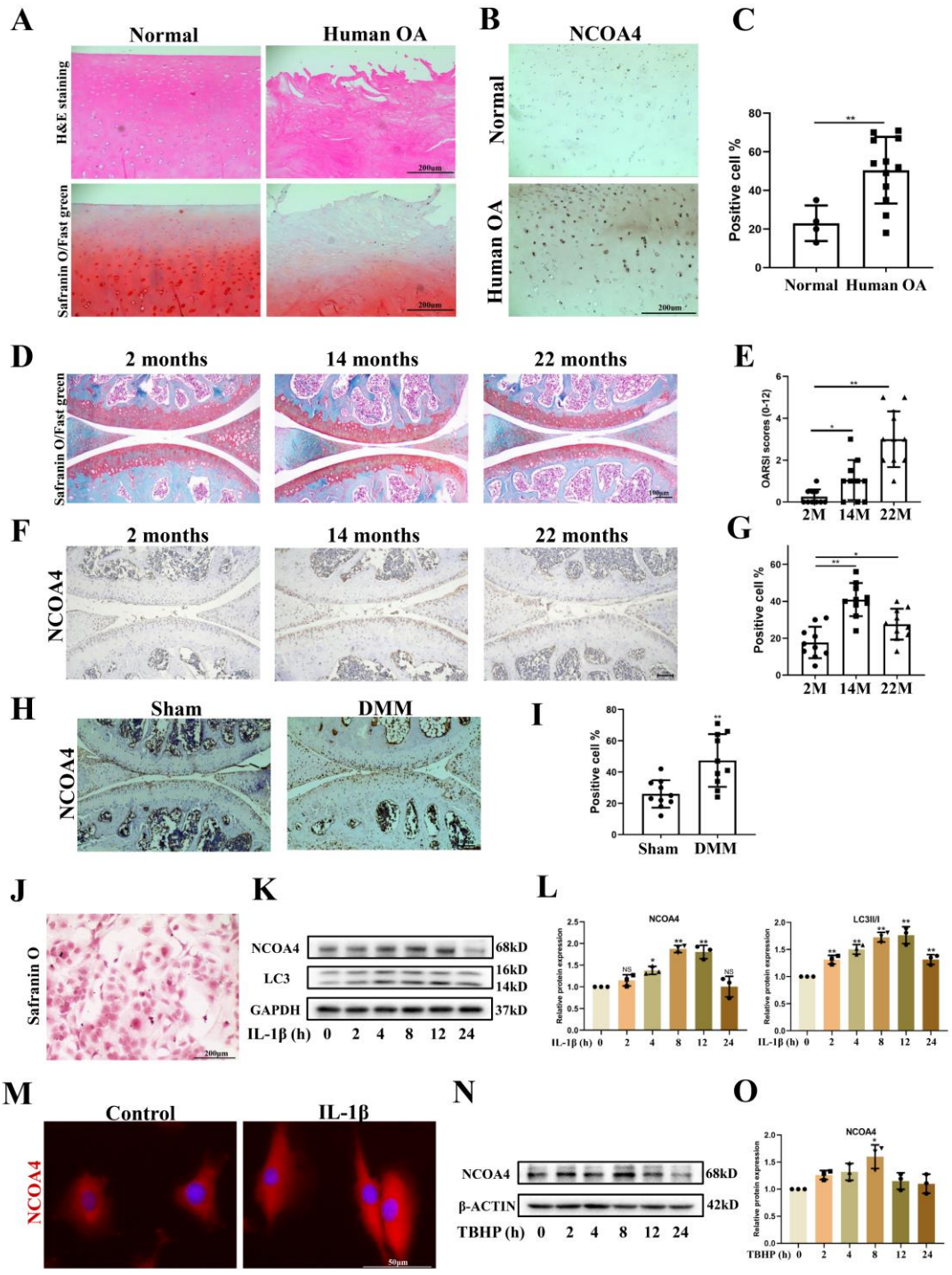

Fig. 1. The expression of NCOA4 in OA cartilage and primary chondrocytes. (A, B) Representative images of H&E, Safranin O/fast green staining and IHC of NCOA4 in human OA cartilage and normal cartilage (scale bars: 200 μm). (C) Quantitative analysis of NCOA4-positive chondrocytes as a proportion of the total chondrocytes (control group, n = 4; OA group, n = 12). (D) Representative images of Safranin

O/Fast green staining of cartilage of 2-month-aged, 14-month-aged, and 22-month-aged mice and (E) OARSI scores of three groups. (F) Representative images of IHC of NCOA4 in cartilage from the above groups and (G) quantitative analysis of NCOA4-positive chondrocytes/total chondrocytes (scale bars: 100 μm, n = 10 each group). (H) Representative images of IHC of NCOA4 and (I) quantitative analysis of NCOA4-positive chondrocyte in cartilage from sham group and DMM group (scale bars: 200 μm, n = 10 each group). (J) The morphology of primary chondrocyte via Safranin O staining (scale bars: 200 μm). (K, N) Western blot results and (L, O) semi-quantitative analysis of band density in chondrocytes treated with IL-1β or TBHP for 0, 2, 4, 8,12, and 24 h, n = 3. (M) Representative images of IF staining for NCOA4 expression and distribution in chondrocytes treated with IL-1β for 12 h (scale bars: 50 μm). Data are presented as the mean ± SD, * $P < 0.05$, ** $P < 0.01$.

NCOA4 contributed to ferroptosis and OA-like phenotype of chondrocytes

Given that our previous finding that chondrocyte ferroptosis contributes to OA pathogenesis[13] and emerging report that NCOA4 can regulate epithelial cell ferroptosis[17], we further explore the functional role of NCOA4 in chondrocyte ferroptosis. Firstly, the knockdown efficiency of *Ncoa4* using RNA interference was confirmed by qRT-PCR and western blot (Fig. S1A-C). Primary chondrocytes were subjected to IL-1β stimulation, which can induce a phenotype of ferroptosis and extracellular matrix (ECM) degradation. Compared with IL-1β treated group, knockdown of NCOA4 significantly inhibited ferroptotic process, as evidenced by the reduced expression of ferroptosis markers, including Acyl-CoAsynthetase long chain family member 4 (ACSL4), and P53, and increased expression of glutathione peroxidase 4 (GPX4) following IL-1β treatment (Fig. 2A-B). Ferroptosis is a ferrous

ions-dependent cellular event[5]. Therefore, we investigated alteration of ferrous ions levels using a ferric ion probe and the results showed that ferrous ions level was reduced in *Ncoa4*-knockdown chondrocytes compared to IL-1β treated chondrocytes (Fig. 2C). Lipid peroxidation is a hallmark of ferroptosis[26]. We then examined the level of lipid peroxidation and found reduced levels of lipid reactive oxygen species (ROS) and MDA while elevated GSH levels in *Ncoa4*-knockdown chondrocytes under IL-1β treatment (Fig. 2D, F, G). The TEM results revealed smaller mitochondria and loss of mitochondrial crista in IL-1β treated chondrocyte, while knockdown of *Ncoa4* could partially reverse this phenomenon (Fig. 2E). Furthermore, we examined cell viability and found that knockdown of *Ncoa4* significantly suppressed IL-1β-induced loss of chondrocyte viability (Fig. 2H). The most important function of chondrocyte is to maintain ECM homeostasis[27]. Thus, the alteration of ECM metabolism was further examined by western blot and the data showed that *Ncoa4* knockdown significantly restored ECM homeostasis, revealed by the reduced expression of catabolic markers, including A Disintegrin and Metalloproteinase with Thrombospondin Motifs 5 (ADAMTS5), matrix metallopeptidase 13 (MMP13) and metallopeptidase 3 (MMP3), and enhanced expression of anabolic marker, collagen type II alpha 1 chain (COL2A1), under IL-1β treatment. Additionally, IL-1β-induced inflammatory response was attenuated in *Ncoa4*-knockdown chondrocytes, exhibited by reduced expression of inducible nitric oxide synthase (iNOS) and cyclooxygenase-2 (COX2) (Fig. 2I-L). To further confirm the above data, we investigate the role of upregulated NCOA4 in chondrocytes. Western blot results revealed that the expression of NCOA4 was efficiently upregulated in chondrocytes by *Ncoa4*-plasmid transfection, accompanied with downregulated expression of ferritin heavy chain 1 (FTH1) (Fig. S2A-B). As expected, increased expression of P53 and reduced

expression of GPX4 and COL2A1 were observed in *Ncoa4*-overexpressing chondrocytes (Fig. S2C-D). Collectively, these results suggest that NCOA4 contributes to ferroptosis and OA-like phenotype of chondrocytes.

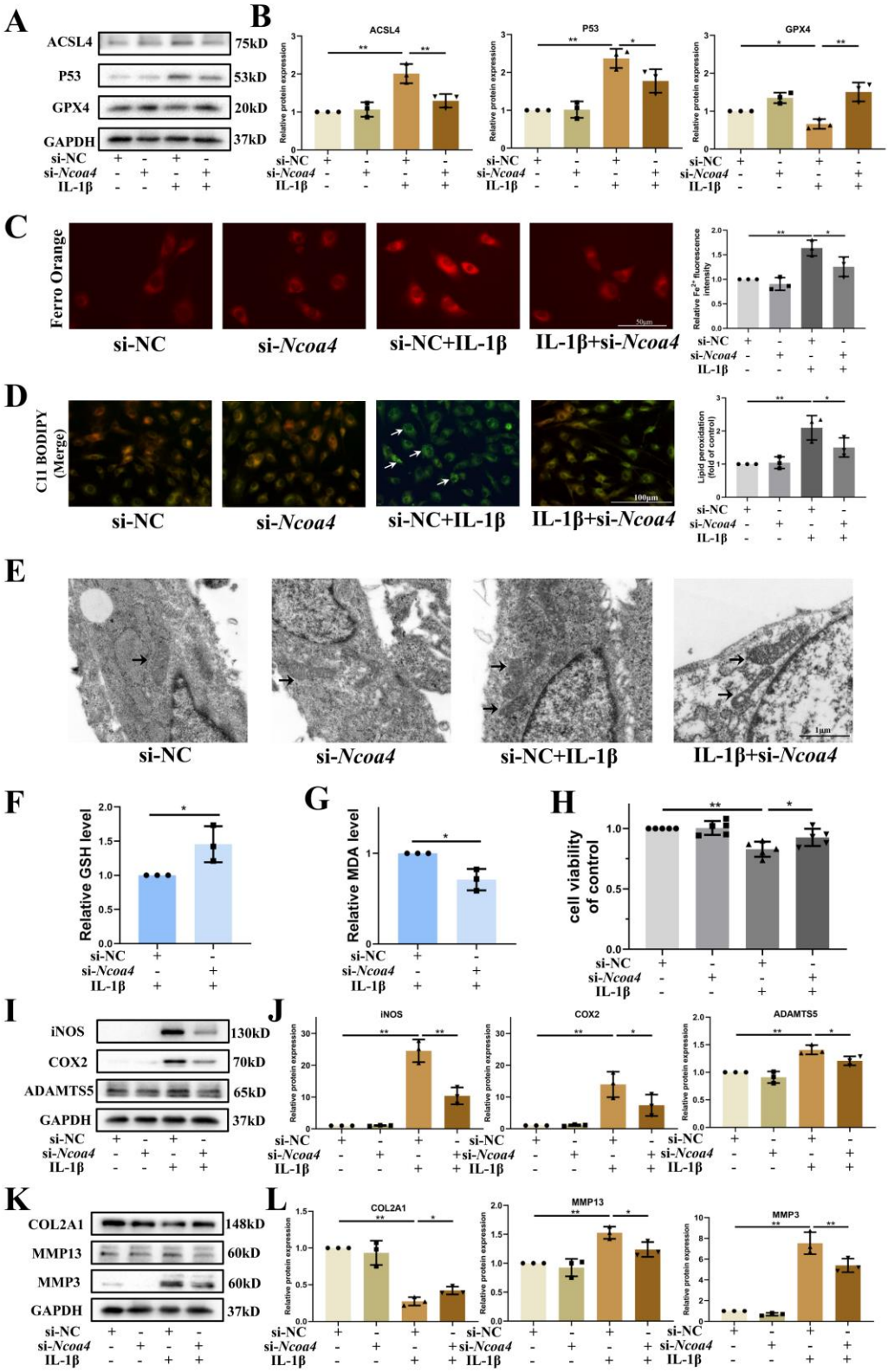

Fig. 2. The impact of NCOA4 on chondrocyte ferroptosis and ECM degradation. (A, B) Western blot analysis of ACSL4, P53, and GPX4 expression in primary chondrocytes transfected with scrambled siRNA or *Ncoa4* siRNA following IL-1β induction for 48 h. (C, D) Representative staining for ferrous ions and lipid ROS in the indicated group and statistical analysis of fluorescence intensity (ferrous ions) and lipid peroxidation (green/red ratio). (E) Representative TEM images for mitochondria in chondrocytes transfected with siRNA negative control (NC) or *Ncoa4* siRNA following IL-1β induction for 48 h, the black arrows indicate mitochondria in chondrocytes. (F, G) Relative levels of MDA and GSH in chondrocytes treated as the indicated for 48 h. (H) Relative viability of chondrocytes transfected with siRNA NC or si-*Ncoa4* following IL-1β induction for 72 h. (I, K) Western blot analysis of iNOS, COX2, ADAMTS5, MMP13, MMP3 and COL2A1 expression in chondrocytes transfected with NC or siNCOA4 following IL-1β induction for 48 h and (J, L) semi-quantitative analysis of band density. Data are presented as the mean ± SD, * $P < 0.05$, ** $P < 0.01$.

NCOA4 accelerated development of post-traumatic OA

We further assessed the requirement of NCOA4 during the development of OA in mice. The AAV9-NCOA4 was injected into articular cavity to achieve the overexpression of NCOA4 in cartilage (Fig. 3A). The results showed that the AAV9 could efficiently infect the chondrocyte of articular cartilage for 10 weeks at least (positive cell: 68.67 ± 6.96%) (Fig. S3A-B). AAV9-NCOA4 also significantly increased the number of NCOA4-chondrocytes in cartilage compared with the control (Fig. 3B-C). The mice were subjected to DMM surgery or sham operation from two weeks after the first injection of AAV9. Subsequently, knee tissues were assessed at 8

weeks post DMM surgery. As expected, Safranin O/Fast green staining revealed a feature of cartilage degeneration in mice with DMM surgery, as evidenced by loss of proteoglycan and cartilage erosion with a higher OARSI score compared with that of sham group (Fig. 3D-E). Notably, compared with DMM group, mice injected by AAV9-NCOA4 were more susceptible to DMM-caused degeneration, characterized by a higher OARSI score (Fig. 3D-E). We further determined that whether the NCOA4 overexpression could affect levels of ferroptosis and ECM metabolism markers. The highly expressed MMP13 and COX2 in cartilage of DMM mice were significantly aggravated in AAV-NCOA4-treated mice, however, the expression of COL2A1 and GPX4 were further reduced in cartilage of AAV-NCOA4-treated mice (Fig. 3F-G).

Additionally, we also detected the alteration of subchondral bone, osteophytes, and synovium in four groups. compared with DMM control, AAV9-NCOA4-treated mice after DMM surgery developed larger osteophytes with a higher osteophyte score (Fig. 4A-E). However, there is no significant alteration of subchondral bone and synovitis between AAV-NCOA4-treated group and control group (Fig. S3C-E). Collectively, these results indicate that NCOA4 overexpression in cartilage accelerates cartilage degeneration and osteophyte formation in mice with post-traumatic OA.

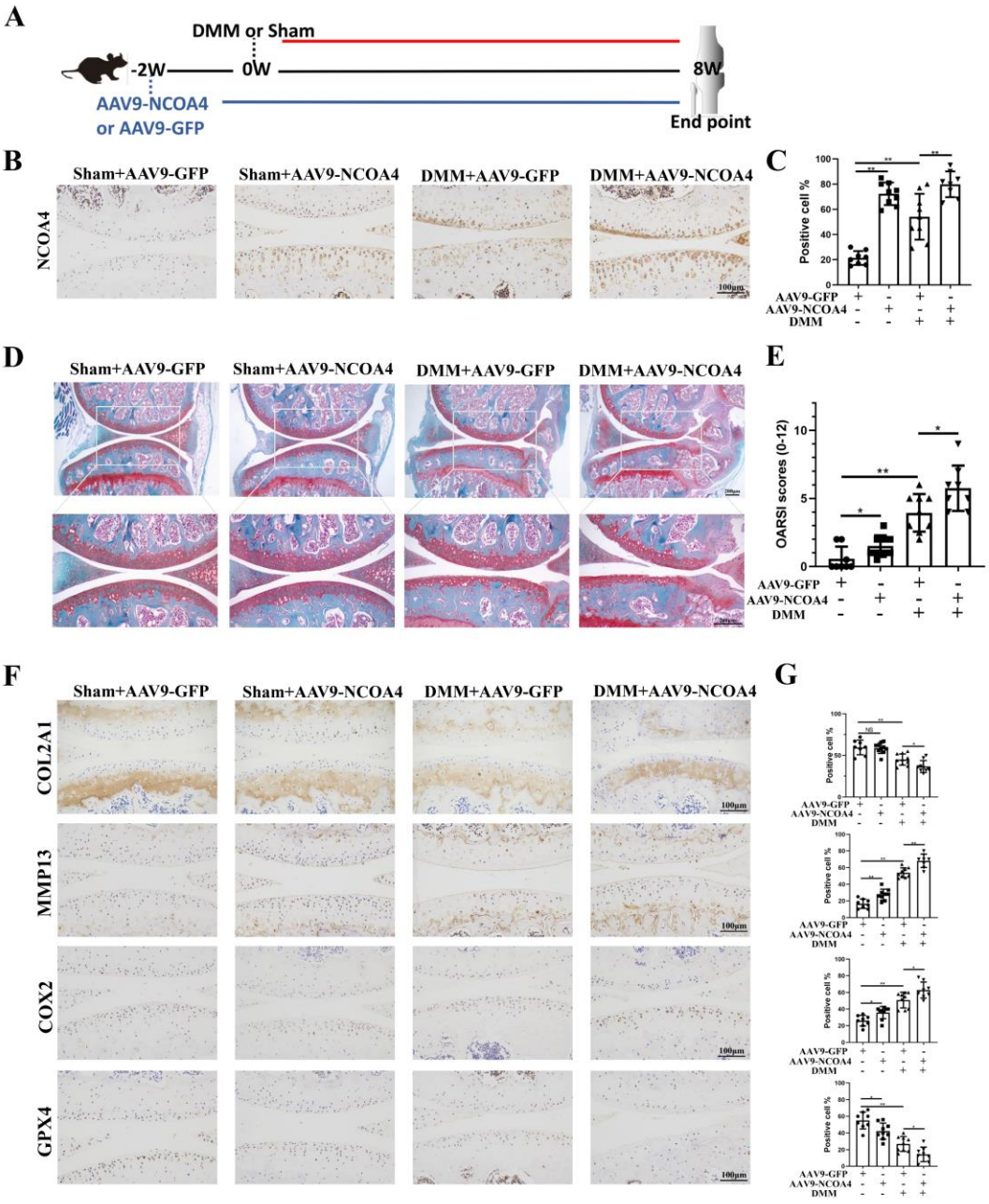

Fig. 3. NCOA4 overexpression exaggerated cartilage degeneration in post-traumatic OA of mice. Eight-week aged mice were randomly divided in four groups and intra-articularly injected AAV9 solution following DMM surgery or sham operation (Sham + AAV9-GFP, n = 8; Sham + AAV9-NCOA4, n = 9; DMM + AAV9-GFP, n = 9; DMM + AAV9-NCOA4, n = 8). Eight weeks after DMM surgery, the knee tissues were collected and then analyzed. (A) Schematic diagram of animal experiment. (B) Representative IHC images of NCOA4-positive chondrocytes in the cartilage of four

groups and (C) quantitative analysis. Scale bar: 100 μm. (D) Safranin O/Fast green staining of joints from four groups and (E) the OARSI scores. Scale bar: 200 μm. (F) Representative IHC images and (G) quantification of COL2A1, MMP13, COX2, and GPX4 in chondrocytes of four groups. Scale bar: 100 μm. Data are shown as mean ± SD. *P<0.05, **P<0.01, NS means no significance.

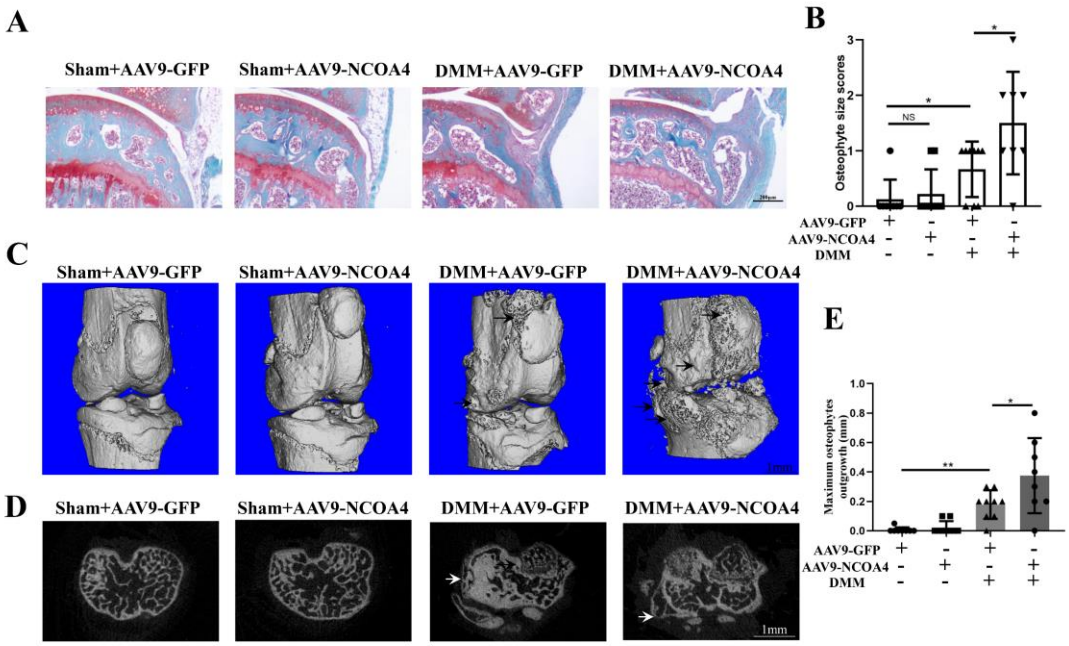

Fig. 4. NCOA4 overexpression promoted osteophyte formation in post-traumatic OA of mice. (A) Safranin O/Fast green staining of joints from four groups and (B) the osteophyte scores. Scale bar: 200 μm. (C) Representative 3D reconstruction images of joints, black arrow indicates osteophyte. Scale bar: 1 mm. (D) The transverse sectional images of tibial plateau and (E) quantitative analysis of maximum osteophyte outgrowth of each sample in four groups, white arrow indicates osteophyte. Scale bar: 1 mm. Data are shown as mean ± SD. *P<0.05, **P<0.01, NS means no significance.

NCOA4 mediated ferritinophagy to regulate ferroptosis of chondrocytes

The current evidence has demonstrated that NCOA4 is a selective cargo receptor of ferritinophagy, which is an autophagic process for ferritin degradation[28], and contributes to ferroptosis[29]. Therefore, we sought to verify that whether the NCOA4-mediated ferritinophagy exists in chondrocytes and involves in chondrocyte ferroptosis. The western blot results revealed that FTH1 degradation was remarkedly reduced after the knockdown of *Ncoa4* in chondrocytes whether exposed to IL-1β or not (Fig. 5A-B). To confirm the interaction between NCOA4 and FTH1, we performed Co-IP experiment and found that NCOA4 could bind to FTH1 (Fig. 5C). To further investigate the occurrence of autophagic influx, chondrocytes were infected with a tandem fluorescent-tagged LC3 (RFP-GFP-LC3) adenovirus. More red and yellow puncta were observed in chondrocytes stimulated by IL-1β compared with the control group, whereas less red and yellow punctas were found in *Ncoa4*-knockdown chondrocytes after IL-1β treatment (Fig. 5D-E), indicating *Ncoa4* deficiency partially blocked the conversion from autophagosome to autophagolysosomes and limited the macroautophagy/autophagy flux. To further confirm whether autophagy level affects ferritinophagy in chondrocytes, the classical inhibitor and activator of autophagy, 3-MA and Rapa, and the inhibitor of the fusion of autophagosome and lysosomes, BafA1, were used. The results showed that 3-MA inhibited NCOA4 expression and restored FTH1 expression while rapamycin treatment exerted opposite effects (Fig. 5F). Additionally, BafA1 treatment promoted LC3 accumulation and simultaneously increased protein level of FTH1 in chondrocytes (Fig. 5G). Consistently, IF analysis revealed that colocalization of endogenous FTH1 and LC3 was increased in IL-1β-treated chondrocytes and further enhanced by BafA1 treatment (Fig. 5H), suggesting the ferritinophagy occurs in IL-1β-treated chondrocytes. Next, we performed the rescue experiment to confirm essential role of ferritinophagy for ferroptosis. The

western blot results showed that knocking down FTH1 partially rescued the expression of ferroptosis markers and ECM metabolism markers in *Ncoa4*-deficiency chondrocytes under IL-1β treatment (Fig. 5I-L). These findings indicate that NCOA4 mediates ferritinophagy and contributes to ferroptosis of chondrocytes.

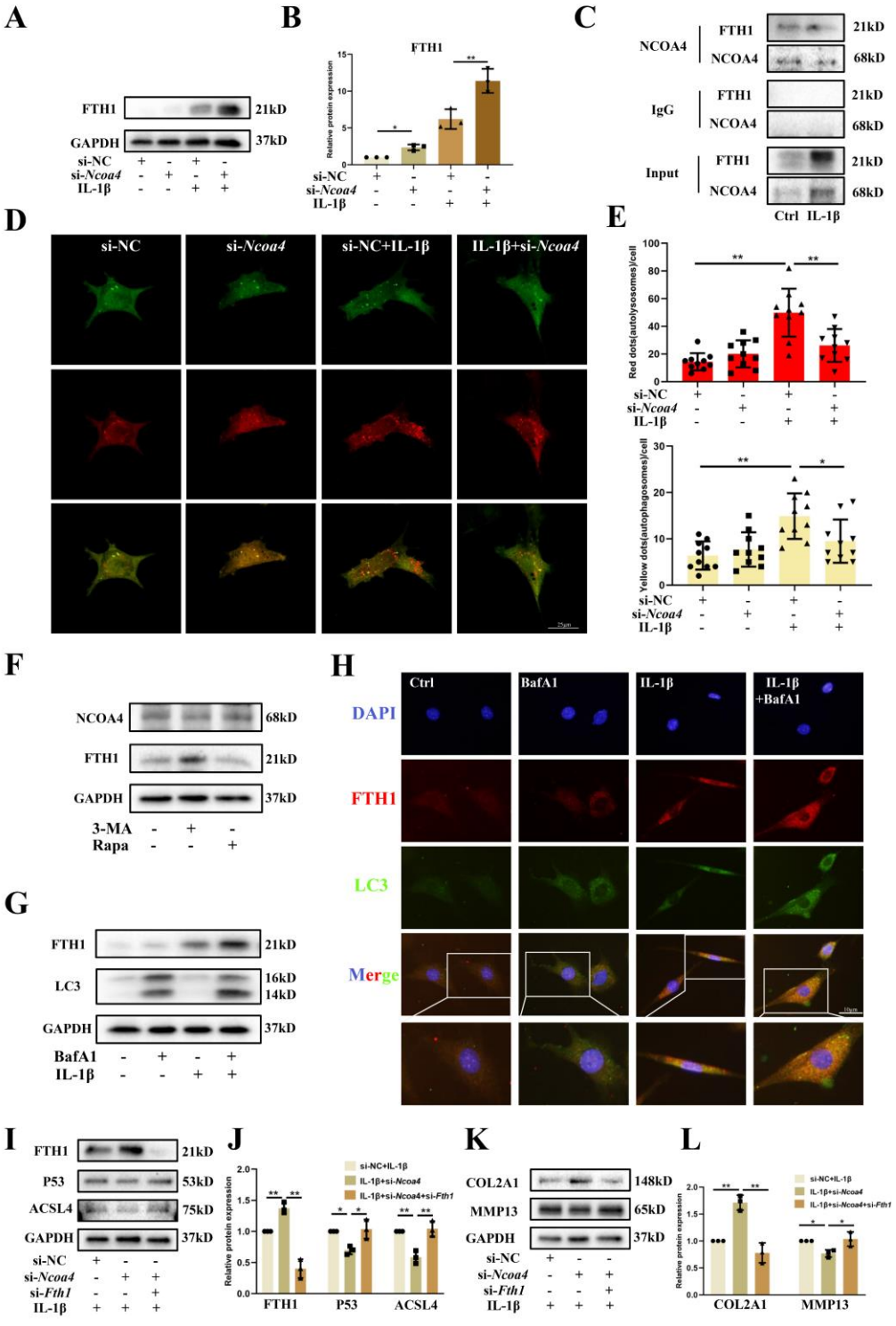

Fig. 5. NCOA4-mediated ferritinophagy in chondrocyte ferroptosis. (A) Chondrocytes were transfected with si-NC or si-*Ncoa4* before IL-1β treatment for 48 h and the FTH1 expression was measured by western blot. (B) The semi-quantitative analysis of FTH1 expression. (C) Chondrocytes were treated with IL-1β for 6 h and the Co-IP analysis of the binding between NCOA4 and FTH1 was shown. (D, E) Chondrocytes were transfected with si-NC or si-*Ncoa4* and then transfected with mRFP-GFP-LC3 adenovirus following IL-1β treatment for 12 h. The representative images of fluorescence were revealed (scale bar: 25 μm) and quantitative analysis of red dots (autolysosomes) and yellow dots (autophagosomes) was performed. (F) 3-MA and rapamycin were used to respectively treat chondrocytes for 12 h and expression of NCOA4 and FTH1 was measured using western blot. Chondrocytes were treated with BafA1 or IL-1β or BafA1 + IL-1β, (G) the expression of LC3 and FTH1 and (H) their colocalization in chondrocytes were determined by western blot and IF (scale bar: 10 μm). Chondrocytes were transfected with si-NC or si-*Ncoa4* or si-*Ncoa4* + si-*Fth1* following IL-1β treatment for 48 h, (I, K) FTH1, P53, ACSL4, COL2A1 and MMP13 expression were examined by western blot and (J, L) semi-quantitative analysis of band density was shown. All bar charts in this figure represent the mean ± SD *P<0.05, **P<0.01.

NCOA4 was upregulated in a JNK-JUN signaling-dependent manner

According to our data that the *Ncoa4* expression was significantly enhanced after a short-time treatment of IL-1β or TBHP (Fig. 6A), we speculated that upregulated expression of NCOA4 during OA development is mainly caused by mRNA synthesis of *Ncoa4*. To clarify the regulatory mechanism for its expression, we firstly used the UCSC Genome Browser database, GeneHancer database (embedded in GeneCards),

and Cistrome Data Browser database to predict the potential transcription factors (TFs) of *Ncoa4* (Fig. 6B) and found that JUN is one of the most possible TFs among three databases. Of note, JUN is closely associated with oxidative stress and OA development[30,31]. To identify whether JUN directly targets the promoter region of *Ncoa4*, we used JASPAR database to predict the potential binding motif, TGACTCA, and then conducted ChIP PCR experiment (Fig. 6C). The results revealed that JUN can bind to the *Ncoa4* promoter at the predictive binding site 1(-893 bp to -887 bp from the upstream of transcriptional start site) (Fig. 6D-F). Next, we performed western blot to further confirm the impact of JUN on the expression of NCOA4. The data showed that the expression of NCOA4 was repressed by the knockdown of JUN in IL-1β-stimulated chondrocytes (Fig. 6F-G). To identify whether JUN mediates downstream cellular events including ferroptosis and ECM degradation via upregulation of NCOA4, we conducted western blot and observed that JUN deficiency notably inhibited ACSL4, P53, and MMP13 expression and promoted protein expression of GPX4 and COL2A1 (Fig. 6H-I). Interestingly, overexpression of NCOA4 significantly promoted the degradation of FTH1 and reversed the above effects (Fig. 6J-K). It has been reported that the activity of JUN is mainly regulated by JNK[32], and multiple compounds can specifically target JNK[33]. Hence, we further explored that whether targeting JNK-JUN axis could protect against chondrocyte ferroptosis and OA pathogenesis. SP600125, a novel and selective JNK inhibitor that can substantially suppress activity of JUN[34], was applied in our study. Notably, inhibition of JNK with SP600125 repressed activity of JUN, expression of NCOA4, degradation of FTH1, and further attenuated ferroptosis process and ECM degradation in chondrocytes (Fig. 6L-P). To demonstrated the essential role of NCOA4 in the effect of SP600125, we performed the rescue experiment and found that

overexpression of NCOA4 significantly suppressed SP600125' effect in IL-1β-stimulated chondrocytes, as evidenced by downregulated expression of FTH1, COL2A1, and GPX4 (Fig. 6Q-R). Collectively, these results demonstrates that NCOA4 is upregulated in a JNK-JUN signaling-dependent manner during OA development.

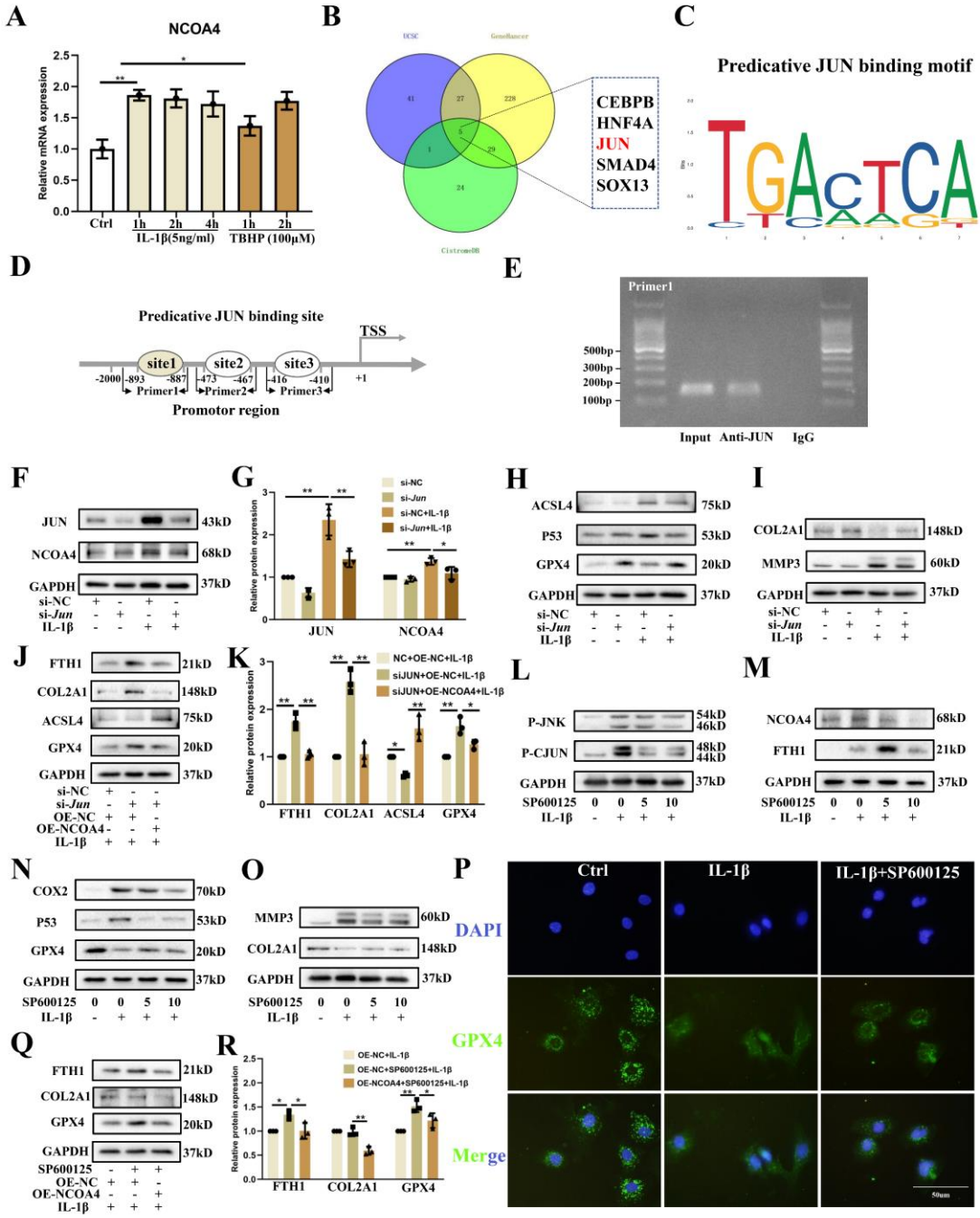

Fig. 6. The regulatory mechanism for NCOA4 expression and the role of JNK-JUN-

NCOA4 axis in chondrocyte ferroptosis. (A) the mRNA levels of *Ncoa4* in chondrocytes treated with IL-1β or TBHP. (B) Transcription factor, JUN, was screened out by using UCSC Genome Browser database, GeneHancer database (embedded in GeneCards), and Cistrome Data Browser. (C) Predicative binding motif of JUN in promoter of *Ncoa4* by using JASPAR database. (D) Schematic of the predictive binding site of JUN at the promoter. (E) Chondrocytes were exposed to IL-1β for 30 min and the ChIP assay was conducted. JUN binding to promoter of *Ncoa4* was determined by PCR. JUN antibody was used for immunoprecipitation with normal IgG as the negative control and input as loading control. (F, H, I) Western blot results of JUN, NCOA4, ACSL4, P53, GPX4, COL2A1 and MMP3 expression in chondrocytes transfected with NC siRNA or JUN siRNA following IL-1β induction for 48 h and (G) semi-quantitative analysis of JUN and NCOA4 expression. Chondrocytes were divided into NC + OE-NC (overexpression-NC plasmid) + IL-1β group, JUN siRNA + OE-NC + IL-1β group and JUN siRNA + OE-NCOA4 (overexpression-*Ncoa4* plasmid) + IL-1β group according to the treatment, (J) western blot results of FTH1, COL2A1, ACSL4 and GPX4 expression and (K) semi-quantitative analysis of the band density. (L) Western blot results of phosphorylation of JNK and JUN in chondrocytes treated with SP600125 (5 and10 μM) following IL-1β induction for 30 min. (M-O) Western blot results of NCOA4, FTH1, COX2, P53, GPX4, COL2A1 and MMP3 in chondrocytes treated with SP600125 (5 and10 μM) following IL-1β induction for 48 h. (P) IF images of GPX4 in chondrocytes treated with SP600125 (5 μM) following IL-1β induction. (Q) Chondrocytes were treated as the indicated and divided into OE-NC + IL-1β, SP600125 + OE-NC + IL-1β, and SP600125 + OE-NCOA4 + IL-1β groups. FTH1, COL2A1 and GPX4 expression were determined by western blot and semi-quantitative analysis was shown in (R). All

bar charts in this figure represent the mean ± SD *P<0.05, **P<0.01.

Administration of SP600125 attenuated post-traumatic OA via NCOA4

Based on the above finding, we applied SP600125 to further illustrate the therapeutic effects of targeting JNK-JUN-NCOA4 axis on OA progression. DMM surgery was performed on the knee of male mice to establish the post-traumatic OA model. To avoid possible system effect caused by SP600125, we chose a local administration of SP600125 by the intra-articular injection. A week after DMM surgery, SP600125 or vehicle solution was injected into articular cavity once a week in an 8-week period (Fig. 7A). The IHC results exhibited less NCOA4-positive chondrocytes in cartilage of DMM mice injected with SP600125 compared with DMM mice (Fig. 7B-C), indicating inhibitory effect of SP600125 on NCOA4 expression. Furthermore, Safranin O/Fast green staining showed that the administration of SP600125 (1 mg/kg) led to the significant attenuation of cartilage erosion, validated by a lower OARSI score compared with DMM mice (Fig. 7D-E). Consistently, increased protein levels of MMP13 and COX2, together with reduced expression of GPX4 in cartilage of DMM mice, were greatly repressed by SP600125 treatment (Fig. 7F-G). In addition, subchondral bone and osteophyte formation in these groups were observed and the results showed that osteophyte size was markedly reduced by SP600125 treatment, revealed by a lower osteophyte score as well as a shorter osteophyte outgrowth, compared with that of DMM-surgery group (Fig. 7H–L). However, no significant alteration on subchondral bone mass and synovial inflammation was observed between DMM mice and SP600125-treated DMM mice (Fig. S4A-C). Importantly, AAV9-NCOA4 injection partially accelerated the cartilage degeneration with a higher OARSI score compared with that of SP600125 treatment

group. In addition, AAV9-NCOA4 injection caused higher expression of NCOA4, MMP13, and COX2, lower expression of GPX4 and COL2A1 in cartilage compared with that of SP600125 treatment group (Fig. 7B-G). Besides, the effect of SP600125 on osteophyte formation in DMM mice were abrogated by the injection of AAV9-NCOA4 (Fig. 7H-L). Together, these data demonstrates that the administration of SP600125 could attenuate cartilage degeneration and osteophyte formation in post-traumatic OA mice by inhibiting NCOA4.

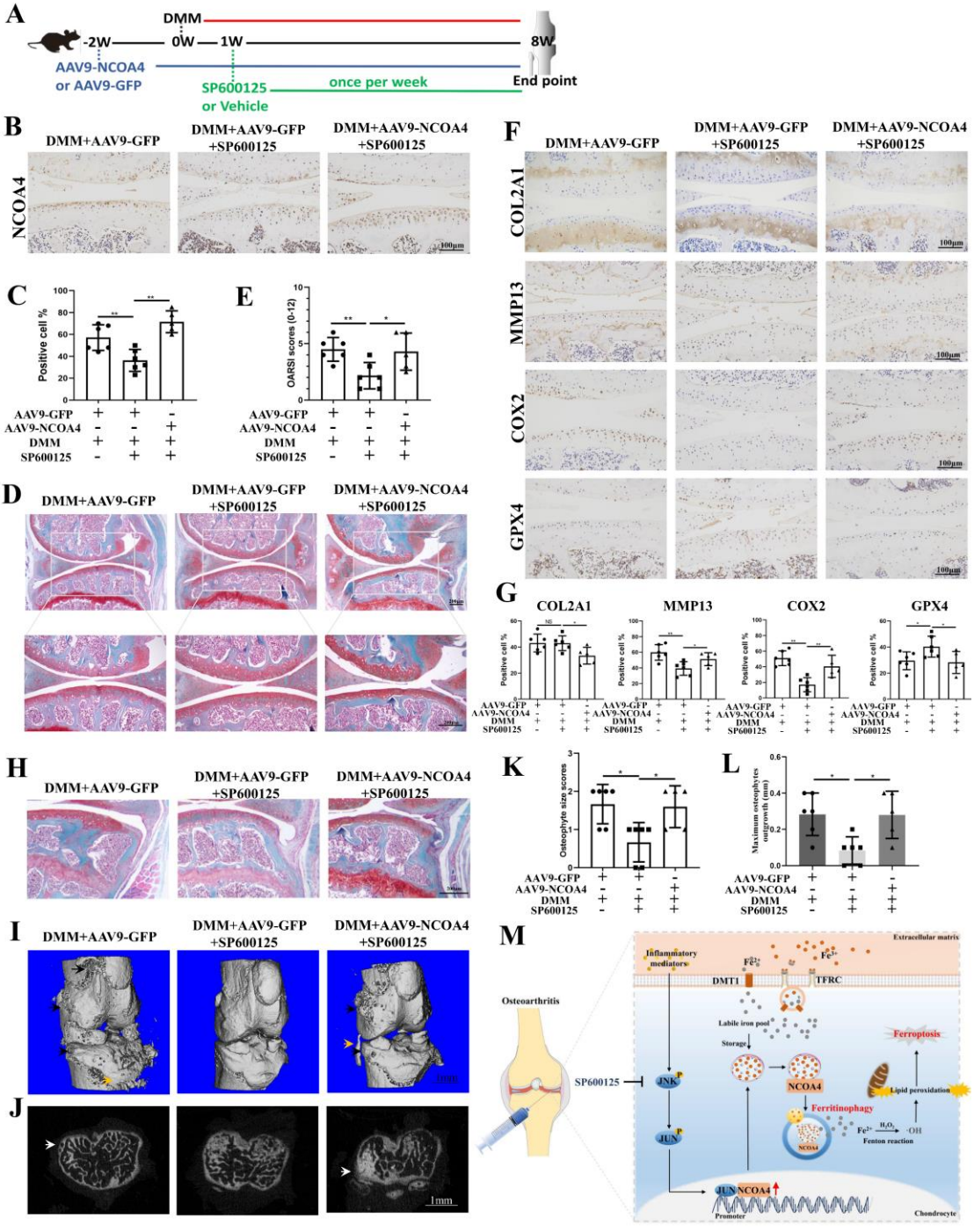

Fig. 7. SP600125 administration alleviated post-traumatic OA of mice via NCOA4. Eight-week aged mice were randomly divided in three groups and intra-articularly injected AAV9 solution followed by DMM surgery with or without SP600125 treatment (DMM + AAV9-GFP, n = 6; DMM + AAV9-GFP + SP600125, n = 6; DMM + AAV9-NCOA4 + SP600125, n = 5). SP600125 (1 mg/kg) solution was intra-articularly injected once per week. Eight weeks after DMM surgery, the knee tissues

were collected and then analyzed. (A) Schematic diagram of animal experiment. (B) Representative IHC images of NCOA4-positive chondrocytes in the cartilage of three groups and (C) quantitative analysis. Scale bar: 100 μm. (D) Safranin O/Fast green staining of joints from three groups and (E) the OARSI scores. Scale bar: 200 μm. (F) Representative IHC images and (G) quantification of COL2A1, MMP13, COX2, and GPX4 in chondrocytes of three groups. Scale bar: 100 μm. (H) Safranin O/Fast green staining of joints from three groups and (K) the osteophyte scores. Scale bar: 200 μm. (I) Representative 3D reconstruction images of joints, black arrow indicates osteophyte, yellow arrow indicates heterotopic ossification. Scale bar: 1 mm. (J) The transverse sectional images of tibial plateau and (L) quantitative analysis of maximum osteophyte outgrowth of each sample in three groups, white arrow indicates osteophyte. Scale bar: 1 mm. (M) The graphic illustration for role of JNK-JUN-NCOA4 axis and ferritinophagy in chondrocyte ferroptosis and OA pathogenesis. Data are shown as mean ± SD. *P<0.05, **P<0.01, NS means no significance.

Discussion

The imbalance of iron homeostasis is involved in multiple ageing related diseases while its role in OA development is largely unknown. Our previous studies focus on inflammatory mediators and iron homeostasis in OA pathogenesis[13,35]. Thus, we sought to find out a bond between these two critical pathologic factors in this study. We identified NCOA4 as a bridge connecting inflammatory mediator and chondrocyte ferroptosis in OA pathogenesis. IL-1β could upregulate NCOA4 in a JNK-JUN-dependent manner and thereby promote NCOA4-mediated ferritinophagy. Autophagy-mediate FTH1 degradation releases excessive iron ions, which causes lipid peroxidation and ECM degradation, eventually resulting in chondrocyte ferroptosis

and cartilage degeneration. Therefore, maintaining cellular iron levels by inhibition of JNK-CJUN-NCOA4 axis may be a novel therapeutic strategy for OA (Fig. 7M).

NCOA4 has emerged as a selective cargo receptor for ferritinophagy that mediates autophagic degradation of ferritin[28] and ferritinophagy has recently been identified as a vital mechanism for regulating iron-dependent ferroptosis[29]. Yoshida and his collogues have demonstrated that NCOA4-mediated ferritinophagy is initiated in bronchial epithelial cells in response to cigarette smoke exposure and involved in chronic obstructive pulmonary disease pathogenesis[17]. However, its role in chondrocyte ferroptosis and OA pathogenesis has not been illustrated. In our study, NCOA4 was remarkedly upregulated in OA chondrocytes. Additionally, it was confirmed that NCOA4-mediated ferritinophagy existed in chondrocyte and contributed to chondrocyte ferroptosis. One of important finding in this study is that NCOA4 deficiency could attenuate chondrocyte ferroptosis and ECM degradation while NCOA4 overexpression exacerbated the development of post-traumatic OA, which suggests an important role of NCOA4-ferroptosis in OA pathogenesis. Interestingly, we found that IL-1β increased protein level of FTH1 accompanied with increased expression of NCOA4. In fact, some studies have shown that inflammation-related mediators, including IL-1β and lipopolysaccharide, could upregulate FTH1 expression[36,37]. Moreover, Ferritin has also been considered as an acute-phase reactive protein and is over-produced when the infection or inflammation response occurs in the body[38]. These evidence suggests that Ferritin or FTH1 level is closely associated with inflammatory mediators and could be regulated by IL-1β. We speculate that increased level of FTH1 in inflammation condition is a stress mechanism to mediate iron distribution and protect cells by storing more iron ions.

Our previous study and other study demonstrate that IL-1β could promote excessive iron influx in chondrocytes[35,39]. These results indicate that a large amount of iron ions could be stored in ferritin under the inflammatory condition. In this case, aberrant expression of NCOA4 would cause severe release of iron ions through the degradation of excessive FTH1, suggesting NCOA4 may act as a key role in IL-1β-FTH1-ferritinophagy axis in chondrocytes.

The intracellular abundance of NCOA4 is crucial for degree of ferritinophagy and ferroptosis. Therefore, it is important to further explore the regulatory mechanism of NCOA4 expression. Although the previous evidence has shown that NCOA4 expression can be affected by some agents or molecules, such as cigarette smoke[17], ionizing radiation[40], and TBHP[41], it is far from elucidating regulatory mechanism of NCOA4 expression. In this study, we found that upregulated expression of NCOA4 in response to pathologic conditions (IL-1β or TBHP) was governed by mRNA synthesis. To identify direct transcription factor for *Ncoa4*, we consulted three databases and screened out JUN as potential transcription factor. Importantly, we demonstrated the direct binding between transcription factor JUN and the promoter of *Ncoa4*. Furthermore, inhibition of JUN-JUN axis suppressed ferritin degradation and ultimately alleviated chondrocyte ferroptosis and ECM degradation. Of note, we demonstrated the protective effect of SP600125 against OA progression by the downregulation of NCOA4. These finding uncovers an indispensable role of JNK-JUN-NCOA4 axis in chondrocyte ferroptosis and OA pathogenesis. Notwithstanding, there is no specific agent targeting the interaction between NCOA4 and FTH1. The development of these agents may provide more precise strategy for OA treatment.

In summary, this study reveals an interaction between iron metabolism and inflammatory factor in OA pathology. NCOA4-mediated ferritinophagy contributed to chondrocyte ferroptosis and aggravated post-traumatic OA. In addition, JNK-JUN axis directly regulated NCOA4 expression and played an important role in IL-1β-induced chondrocyte ferroptosis and OA pathogenesis. Inhibition of JNK-JUN-NCOA4 axis with SP600125 may be a novel strategy for OA treatment.

Declaration of competing interest

The authors confirm that there are no conflicts of interest.

Author contributions

Fengjing Guo: Conceptualization, Project administration, Funding acquisition. Kai Sun: Conceptualization, Visualization, Investigation, Writing - Original Draft. Liangcai Hou: Investigation, Methodology, Visualization. Zhou Guo: Investigation. Genchun Wang: Formal analysis. Jiachao Guo: Resources, Funding acquisition. Jingting Xu: Formal analysis. Xiong Zhang: Investigation. All authors have read and approved the final version of the manuscript.

Funding

This work was supported by the National Natural Science Foundation of China [no. 82172498] and [no. 82102625].

References

[1] M. Yazar, S. Sarban, A. Kocyigit, and U.E. Isikan, Synovial Fluid and Plasma Selenium, Copper, Zinc, and Iron Concentrations in Patients with Rheumatoid

778 Arthritis and Osteoarthritis. Biological Trace Element Research 106 (2005) 123-
779 132.
780 [2] L. Kennish, M. Attur, C. Oh, S. Krasnokutsky, J. Samuels, J.D. Greenberg, X.
781 Huang, and S.B. Abramson, Age-dependent ferritin elevations and HFE C282Y
782 mutation as risk factors for symptomatic knee osteoarthritis in males: a
783 longitudinal cohort study. BMC Musculoskeletal Disorders 15 (2014) 8-8.
784 [3] L.H. Burton, L.B. Radakovich, A.J. Marolf, and K.S. Santangelo, Systemic iron
785 overload exacerbates osteoarthritis in the strain 13 guinea pig. Osteoarthritis and
786 Cartilage 28 (2020) 1265-1275.
787 [4] A.R. Bogdan, M. Miyazawa, K. Hashimoto, and Y. Tsuji, Regulators of Iron
788 Homeostasis: New Players in Metabolism, Cell Death, and Disease. Trends in
789 Biochemical Sciences 41 (2016) 274-286.
790 [5] S.J. Dixon, K.M. Lemberg, M.R. Lamprecht, R. Skouta, E.M. Zaitsev, C.E.
791 Gleason, D.N. Patel, A.J. Bauer, A.M. Cantley, W.S. Yang, B.R. Morrison, and
792 B.R. Stockwell, Ferroptosis: an iron-dependent form of nonapoptotic cell death.
793 Cell 149 (2012) 1060-1072.
794 [6] L. Mahoney-Sanchez, H. Bouchaoui, I. Boussaad, A. Jonneaux, K. Timmerman,
795 O. Berdeaux, S. Ayton, R. Krüger, J.A. Duce, D. Devos, and J. Devedjian, Alpha
796 synuclein determines ferroptosis sensitivity in dopaminergic neurons via
797 modulation of ether-phospholipid membrane composition. Cell Reports 40 (2022)
798 111231.
799 [7] U. Gupta, S. Ghosh, C.T. Wallace, P. Shang, Y. Xin, A.P. Nair, M. Yazdankhah,

A. Strizhakova, M.A. Ross, H. Liu, S. Hose, N.A. Stepicheva, O. Chowdhury, M. Nemani, V. Maddipatla, R. Grebe, M. Das, K.L. Lathrop, J. Sahel, J.S. Zigler, J. Qian, A. Ghosh, Y. Sergeev, J.T. Handa, C.M. St. Croix, and D. Sinha, Increased LCN2 (lipocalin 2) in the RPE decreases autophagy and activates inflammasome-ferroptosis processes in a mouse model of dry AMD. Autophagy (2022) 1-20.

[8] Z. Tang, Y. Ju, X. Dai, N. Ni, Y. Liu, D. Zhang, H. Gao, H. Sun, J. Zhang, and P. Gu, HO-1-mediated ferroptosis as a target for protection against retinal pigment epithelium degeneration. Redox Biology 43 (2021) 101971.

[9] D. Tang, X. Chen, R. Kang, and G. Kroemer, Ferroptosis: molecular mechanisms and health implications. Cell Research 31 (2021) 107-125.

[10] K. Sun, Z. Guo, L. Hou, J. Xu, T. Du, T. Xu, and F. Guo, Iron homeostasis in arthropathies: From pathogenesis to therapeutic potential. Ageing Research Reviews 72 (2021) 101481.

[11] A. Ostalowska, E. Birkner, M. Wiecha, S. Kasperczyk, A. Kasperczyk, D. Kapolka, and A. Zon-Giebel, Lipid peroxidation and antioxidant enzymes in synovial fluid of patients with primary and secondary osteoarthritis of the knee joint. Osteoarthritis Cartilage 14 (2006) 139-45.

[12] K. Sun, X. Jing, J. Guo, X. Yao, and F. Guo, Mitophagy in degenerative joint diseases. Autophagy 17 (2021) 2082-2092.

[13] X. Yao, K. Sun, S. Yu, J. Luo, J. Guo, J. Lin, G. Wang, Z. Guo, Y. Ye, and F. Guo, Chondrocyte ferroptosis contribute to the progression of osteoarthritis. Journal of Orthopaedic Translation 27 (2021) 33-43.

[14] Z. Guo, J. Lin, K. Sun, J. Guo, X. Yao, G. Wang, L. Hou, J. Xu, J. Guo, and F. Guo, Deferoxamine Alleviates Osteoarthritis by Inhibiting Chondrocyte Ferroptosis and Activating the Nrf2 Pathway. Frontiers in Pharmacology 13 (2022) 791376.

[15] Y. Miao, Y. Chen, F. Xue, K. Liu, B. Zhu, J. Gao, J. Yin, C. Zhang, and G. Li, Contribution of ferroptosis and GPX4's dual functions to osteoarthritis progression. eBioMedicine 76 (2022) 103847.

[16] J.D. Mancias, X. Wang, S.P. Gygi, J.W. Harper, and A.C. Kimmelman, Quantitative proteomics identifies NCOA4 as the cargo receptor mediating ferritinophagy. Nature 509 (2014) 105-109.

[17] M. Yoshida, S. Minagawa, J. Araya, T. Sakamoto, H. Hara, K. Tsubouchi, Y. Hosaka, A. Ichikawa, N. Saito, T. Kadota, N. Sato, Y. Kurita, K. Kobayashi, S. Ito, H. Utsumi, H. Wakui, T. Numata, Y. Kaneko, S. Mori, H. Asano, M. Yamashita, M. Odaka, T. Morikawa, K. Nakayama, T. Iwamoto, H. Imai, and K. Kuwano, Involvement of cigarette smoke-induced epithelial cell ferroptosis in COPD pathogenesis. Nature Communications 10 (2019) 3145.

[18] S. Shen, Y. Yang, P. Shen, J. Ma, B. Fang, Q. Wang, K. Wang, P. Shi, S. Fan, and X. Fang, circPDE4B prevents articular cartilage degeneration and promotes repair by acting as a scaffold for RIC8A and MID1. Annals of the Rheumatic Diseases 80 (2021) 1209-1219.

[19] S.S. Glasson, T.J. Blanchet, and E.A. Morris, The surgical destabilization of the medial meniscus (DMM) model of osteoarthritis in the 129/SvEv mouse.

Osteoarthritis and Cartilage 15 (2007) 1061-1069.

[20] L. Chen, J. Zhang, Y. Zou, F. Wang, J. Li, F. Sun, X. Luo, M. Zhang, Y. Guo, Q. Yu, P. Yang, Q. Zhou, Z. Chen, H. Zhang, Q. Gong, J. Zhao, D.L. Eizirik, Z. Zhou, F. Xiong, S. Zhang, and C. Wang, Kdm2a deficiency in macrophages enhances thermogenesis to protect mice against HFD-induced obesity by enhancing H3K36me2 at the Pparg locus. Cell Death & Differentiation 28 (2021) 1880-1899.

[21] S.S. Glasson, M.G. Chambers, W.B. Van Den Berg, and C.B. Little, The OARSI histopathology initiative – recommendations for histological assessments of osteoarthritis in the mouse. Osteoarthritis and Cartilage 18 (2010) S17-S23.

[22] M.A. Rowe, L.R. Harper, M.A. McNulty, A.G. Lau, C.S. Carlson, L. Leng, R.J. Bucala, R.A. Miller, and R.F. Loeser, Reduced Osteoarthritis Severity in Aged Mice With Deletion of Macrophage Migration Inhibitory Factor. Arthritis & Rheumatology 69 (2017) 352-361.

[23] J.S. Lewis, W.C. Hembree, B.D. Furman, L. Tippets, D. Cattel, J.L. Huebner, D. Little, L.E. DeFrate, V.B. Kraus, F. Guilak, and S.A. Olson, Acute joint pathology and synovial inflammation is associated with increased intra-articular fracture severity in the mouse knee. Osteoarthritis and Cartilage 19 (2011) 864-873.

[24] M. Rahmati, G. Nalesso, A. Mobasheri, and M. Mozafari, Aging and osteoarthritis: Central role of the extracellular matrix. Ageing Res Rev 40 (2017) 20-30.

[25] C.L. Blaker, E.C. Clarke, and C.B. Little, Using mouse models to investigate the

pathophysiology, treatment, and prevention of post-traumatic osteoarthritis. Journal of Orthopaedic Research 35 (2017) 424-439.

[26] X. Chen, J. Li, R. Kang, D.J. Klionsky, and D. Tang, Ferroptosis: machinery and regulation. Autophagy 17 (2021) 2054-2081.

[27] T. Komori, Molecular Processes in Chondrocyte Biology. International Journal of Molecular Sciences 21 (2020) 4161.

[28] J.D. Mancias, X. Wang, S.P. Gygi, J.W. Harper, and A.C. Kimmelman, Quantitative proteomics identifies NCOA4 as the cargo receptor mediating ferritinophagy. Nature 509 (2014) 105-109.

[29] W. Hou, Y. Xie, X. Song, X. Sun, M.T. Lotze, H.J. Zeh, R. Kang, and D. Tang, Autophagy promotes ferroptosis by degradation of ferritin. Autophagy 12 (2016) 1425-1428.

[30] J. Rhee, S. Park, S. Kim, J. Kim, C. Ha, C. Chun, and J. Chun, Inhibition of BATF/JUN transcriptional activity protects against osteoarthritic cartilage destruction. Annals of the Rheumatic Diseases 76 (2017) 427-434.

[31] B.R. Gehi, K. Gadhave, V.N. Uversky, and R. Giri, Intrinsic disorder in proteins associated with oxidative stress-induced JNK signaling. Cellular and Molecular Life Sciences 79 (2022) 202.

[32] M.A. Bogoyevitch, and B. Kobe, Uses for JNK: the Many and Varied Substrates of the c-Jun N-Terminal Kinases. Microbiology and Molecular Biology Reviews 70 (2006) 1061-1095.

[33] G. Li, W. Qi, X. Li, J. Zhao, M. Luo, and J. Chen, Recent Advances in c-Jun N-

888 Terminal Kinase (JNK) Inhibitors. Current Medicinal Chemistry 28 (2021) 607-
889 627.
890 [34] B.L. Bennett, D.T. Sasaki, B.W. Murray, E.C. O'Leary, S.T. Sakata, W. Xu, J.C.
891 Leisten, A. Motiwala, S. Pierce, Y. Satoh, S.S. Bhagwat, A.M. Manning, and D.W.
892 Anderson, SP600125, An Anthrapyrazolone Inhibitor of Jun N-Terminal Kinase.
893 Proceedings of the National Academy of Sciences - PNAS 98 (2001) 13681-
894 13686.
895 [35] X. Jing, J. Lin, T. Du, Z. Jiang, T. Li, G. Wang, X. Liu, X. Cui, and K. Sun, Iron
896 Overload Is Associated With Accelerated Progression of Osteoarthritis: The Role
897 of DMT1 Mediated Iron Homeostasis. Frontiers in cell and developmental biology
898 8 (2021) 594509-594509.
899 [36] J.T. Rogers, Ferritin translation by interleukin-1and interleukin-6: the role of
900 sequences upstream of the start codons of the heavy and light subunit genes.
901 Blood 87 (1996) 2525.
902 [37] E. Pandur, K. Tamási, R. Pap, G. Jánosa, and K. Sipos, Distinct Effects of
903 Escherichia coli,Pseudomonas aeruginosa and Staphylococcus aureus Cell Wall
904 Component-Induced Inflammation on the Iron Metabolism of THP-1 Cells.
905 International Journal of Molecular Sciences 22 (2021) 1497.
906 [38] K.F. Kernan, and J.A. Carcillo, Hyperferritinemia and inflammation.
907 International Immunology 29 (2017) 401-409.
908 [39] X. Jing, T. Du, T. Li, X. Yang, G. Wang, X. Liu, Z. Jiang, and X. Cui, The
909 detrimental effect of iron on OA chondrocytes: Importance of pro-inflammatory

cytokines induced iron influx and oxidative stress. Journal of Cellular and Molecular Medicine 25 (2021) 5671-5680.

[40] H. Zhou, Y. Zhou, J. Mao, L. Tang, J. Xu, Z. Wang, Y. He, and M. Li, NCOA4-mediated ferritinophagy is involved in ionizing radiation-induced ferroptosis of intestinal epithelial cells. Redox Biology 55 (2022) 102413.

[41] R. Yang, W. Xu, H. Zheng, X. Zheng, B. Li, L. Jiang, and S. Jiang, Involvement of oxidative stress-induced annulus fibrosus cell and nucleus pulposus cell ferroptosis in intervertebral disc degeneration pathogenesis. Journal of cellular physiology 236 (2021) 2725-2739.

1. NCOA4 was highly expressed in cartilage of patients with OA, aged mice, post-traumatic OA mice, and inflammatory chondrocytes.

2. NCOA4-mediated ferritinophagy contributed to chondrocyte ferroptosis and aggravated post-traumatic OA.

3. JNK-JUN axis directly regulated NCOA4 expression and played an important role in IL-1β-induced chondrocyte ferroptosis and OA pathogenesis.

4. Inhibition of JNK-JUN-NCOA4 axis with SP600125 protected against post-traumatic OA, suggesting this axis as a potential target for OA treatment.